

Electronic Supplementary Information (ESI) for

**Defects-rich (Co-CoS<sub>2</sub>)<sub>x</sub>@Co<sub>9</sub>S<sub>8</sub> Nanosheets Derived from  
Monomolecular Precursor Pyrolysis with Excellent Catalytic  
Activity for Hydrogen Evolution Reaction**

Xinwen Zhang,<sup>a,#</sup> Yanyan Liu,<sup>a,#</sup> Jie Gao,<sup>b</sup> Guosheng Han,<sup>a</sup> Meifang Hu,<sup>a</sup> Xianli

Wu,<sup>a,\*</sup> Huaqiang Cao,<sup>c</sup> Xiangyu Wang,<sup>a</sup> and Baojun Li<sup>\*,†</sup>

<sup>a</sup> College of Chemistry and Molecular Engineering, Zhengzhou University, 100 Science Road, Zhengzhou  
450001, P R China

<sup>b</sup> Integrated Analytical Laboratories, 273 Franklin Rd, Randolph, NJ 07869, USA

<sup>c</sup> Department of Chemistry, Tsinghua University, 1 Tsinghua Park, Beijing 100084, P R China

<sup>#</sup> These authors contributed equally to this work.

\* Corresponding Authors. E-mail: lbjfc1@zzu.edu.cn (B.J. Li) and wuxianli@zzu.edu.cn (X.L. Wu).

**Total number of pages: 9**

**Total number of figures: 9**

**Total number of tables: 2**

**Table of Contents**

Experimental Section.....	S2
Figure S1.....	S4
Figure S2.....	S5
Figure S3.....	S5
Figure S4.....	S6
Figure S5.....	S6
Figure S6.....	S7
Figure S7.....	S8
Figure S8.....	S8
Figure S9.....	S9
Table S1.....	S3
Table S2.....	S4

## Supplementary methods

**Materials:** NaOH, anhydrous methanol, absolute ethanol, *n*-heptane, CS<sub>2</sub>, CHCl<sub>3</sub>, and CoSO<sub>4</sub>·7H<sub>2</sub>O were used as raw materials without further purification. Dodecylamine (99%), oleylamine (80-90%) and triphenylphosphine (99%) were purchased from Sigma-Aldrich. Octadecanamine (90%) and *n*-dibutylamine (99%) were obtained from Energy Chemical. All reagents were employed without further purification procedures.

**Synthesis of precursor cobalt dibutyldithiocarbamat (dbdc).** The precursor cobalt dibutyldithiocarbamat, Co(dbdc)<sub>2</sub>, was synthesized according to the follow route. NaOH (2.64 g) and *n*-dibutylamine (11 ml) was added into methanol (80 ml) to form a uniform solution which cooled in an ice water bath. Next, CS<sub>2</sub> (3.96 ml) was added dropwise into the above mixture. Then, the yellow mixture was mixed with an aqueous solution of CoSO<sub>4</sub> (80 ml) containing CoSO<sub>4</sub> ·7H<sub>2</sub>O (9.5 g) and stirred vigorously for overnight. The product was separated by filtering, washed with redistilled water three times, and dried under a vacuum at 30 °C.

**Synthesis of CoS nanosheets through solvothermal method (ST).** Co(Ac)<sub>2</sub>·4H<sub>2</sub>O (2.49 g) and thiourea (1.52 g) were dissolved in redistilled water (60 mL). The solution was transferred to a Teflon-lined autoclave (100 mL) and heated at 180 °C for 12 h. After being cooled to room temperature, the solid was separated by centrifugation, then washed with water and ethanol for three times, and dried at 60 °C. The final product was obtained and denoted as ST-CoS.

**Synthesis of CoS<sub>2</sub> nanosheets through solvothermal method (ST).** Co(NO<sub>3</sub>)<sub>2</sub>·6H<sub>2</sub>O (1.646 g) was dissolved in redistilled water (20 mL). Sulfur powder (1 g) was dispersed in the above solution by ultrasonication. After 30 min, hydrazine monohydrate (16 mL) was added to the solution. The obtained homogeneous solution was transferred to a Teflon-lined steel autoclave (50 mL), and heated to 180 °C for 36 h. After that, the solid was washed with redistilled water, hydrochloric acid and ethanol for three times in turn and then freeze-dried. The obtained powder was heated to 300 °C at a rate of 5 °C·min<sup>-1</sup> and kept for 2 h under N<sub>2</sub> atmosphere. The final product was obtained and denoted as ST-CoS<sub>2</sub>.

**Table S1.** The  $R_s$  values of electrodes containing various samples at an over potential of 0.46 V.

Sample	$R_s$ ( $\Omega$ )	$R_{ct}$ ( $\Omega$ )
DR-Co <sub>9</sub> S <sub>8</sub> -I	10.5	264
DR-Co <sub>9</sub> S <sub>8</sub> -II	12.8	202
DR-Co <sub>9</sub> S <sub>8</sub> -III	10.2	230
DR-Co <sub>9</sub> S <sub>8</sub> -IV	11.1	775
DR-Co <sub>9</sub> S <sub>8</sub> -V	11	1232
DR-Co <sub>9</sub> S <sub>8</sub> -VI	11.4	4667
DR-Co <sub>9</sub> S <sub>8</sub> -VII	11.2	1047
ST-CoS	12.1	8288
ST-CoS <sub>2</sub>	11.3	1743

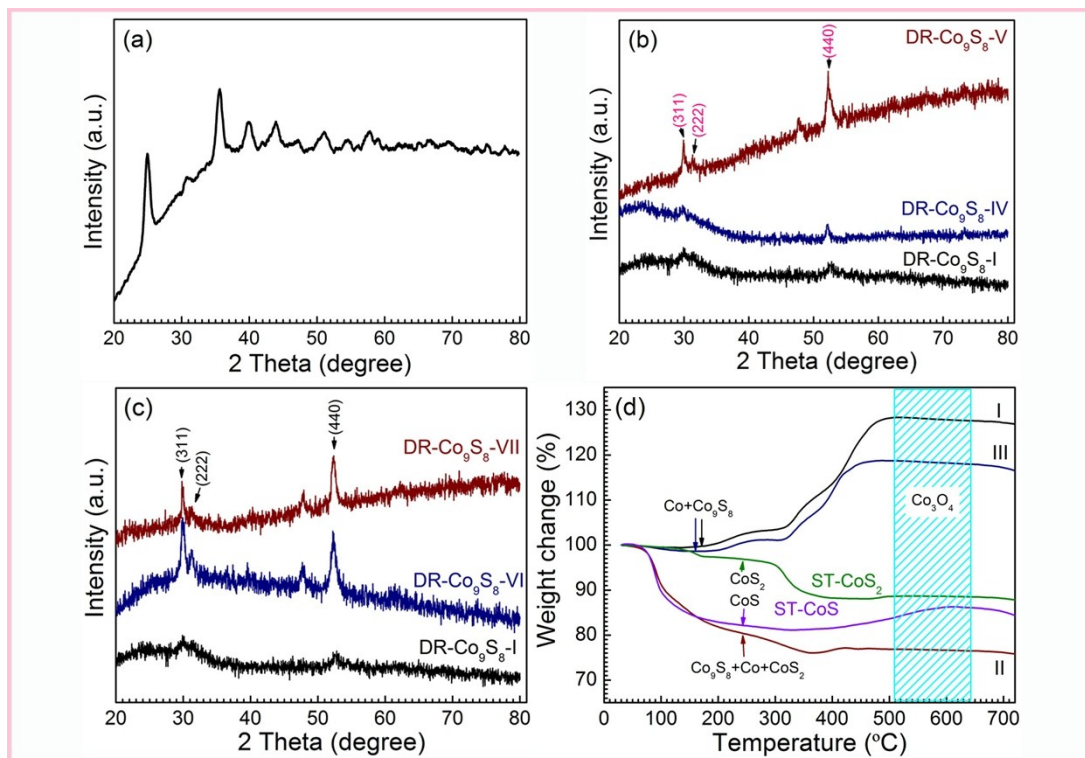


**Figure S1.** (a) XRD patterns of the product of pyrolysis Co(dbdc)<sub>2</sub> in Ar from 25 to 550 °C, (b, c) XRD patterns of DR-Co<sub>9</sub>S<sub>8</sub>-I, IV, V, VI, and VII, and (d) thermogravimetric analysis (TGA) curves of DR-Co<sub>9</sub>S<sub>8</sub>-I, II, III, ST-CoS and ST-CoS<sub>2</sub> in air from 25 to 700 °C.

**Table S2.** The Co content of DR-Co<sub>9</sub>S<sub>8</sub>-I, II, III, ST-CoS and ST-CoS<sub>2</sub> from thermal gravimetric analysis.

Sample	Initial mass (mg)	Final mass (mg)	Co content (mg)
I	4.498	5.7442	4.1996
II	5.433	4.1563	3.0387
III	5.084	5.9957	4.3834
ST-CoS	4.406	3.7866	2.7684
ST-CoS <sub>2</sub>	5.363	4.7457	3.4696

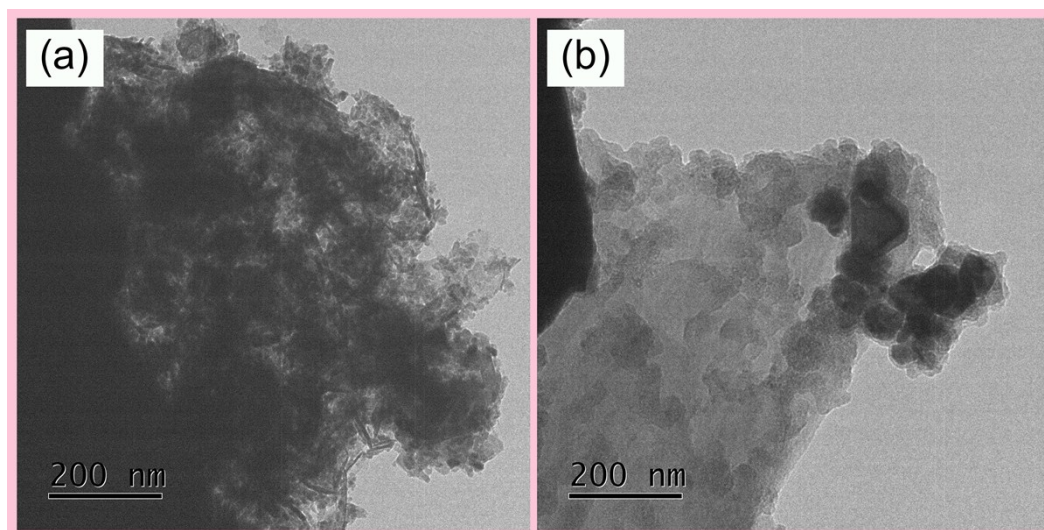


**Figure S2.** TEM images of (a) DR-Co<sub>9</sub>S<sub>8</sub>-IV, and (b) DR-Co<sub>9</sub>S<sub>8</sub>-V.

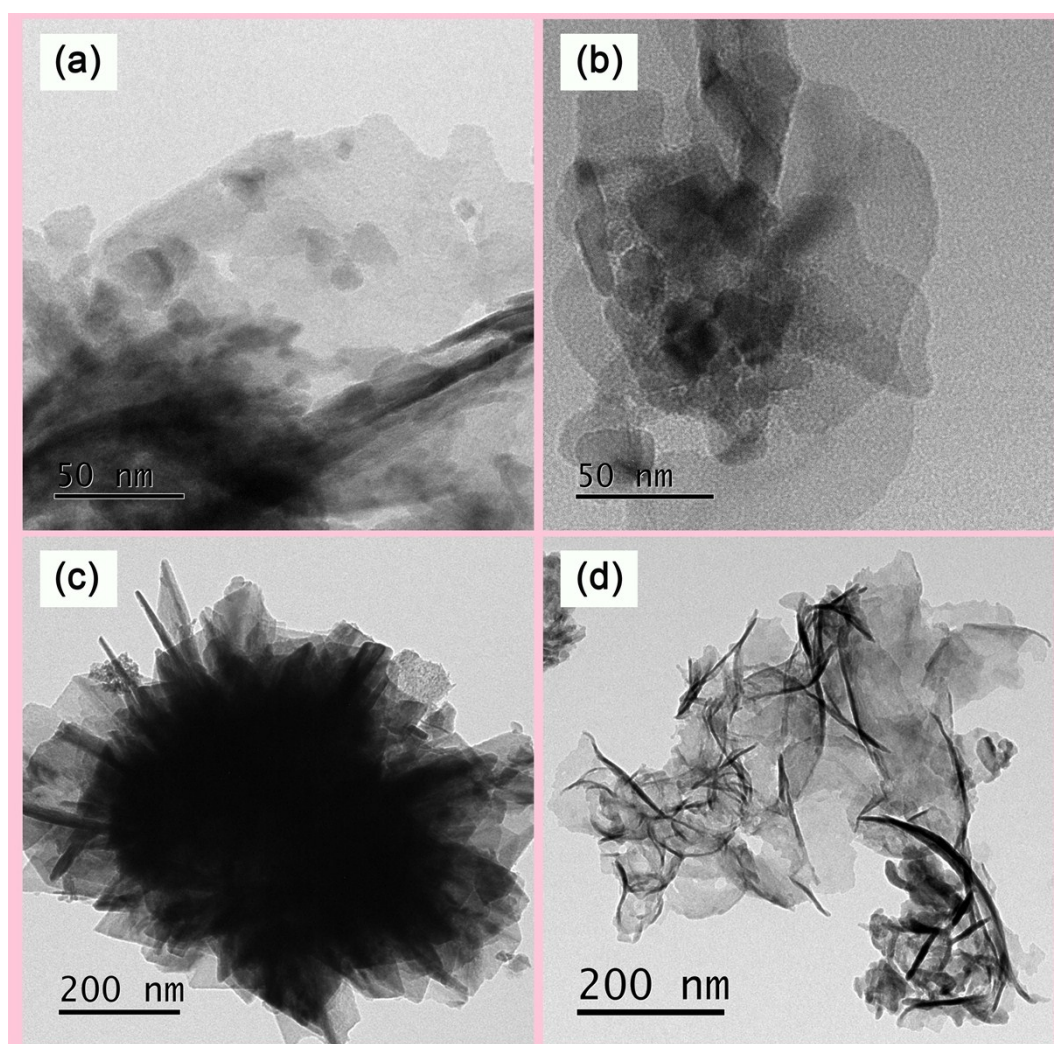


**Figure S3.** TEM images of (a) DR-Co<sub>9</sub>S<sub>8</sub>-VI, (b) DR-Co<sub>9</sub>S<sub>8</sub>-VII, (c) ST-CoS, and (d) ST-CoS<sub>2</sub>.

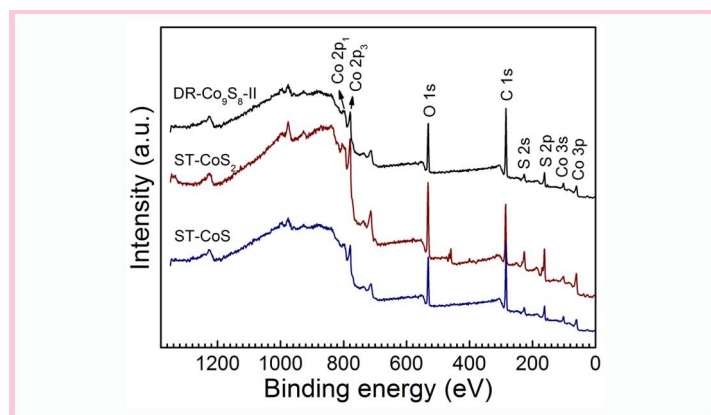


**Figure S4.** XPS survey spectra of DR-Co<sub>9</sub>S<sub>8</sub>-II, ST-CoS and ST-CoS<sub>2</sub>.

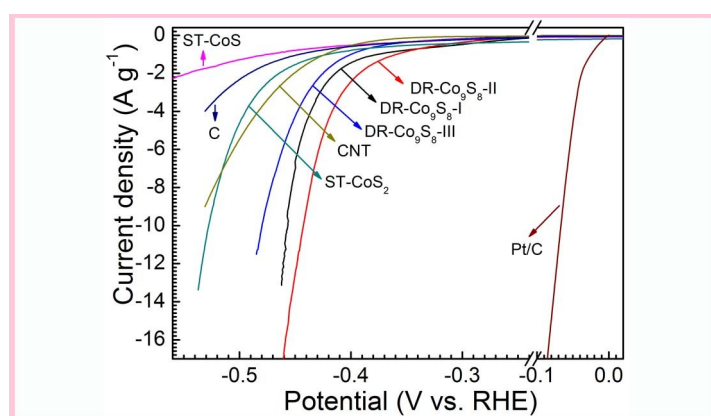


**Figure S5.** Polarization curves of DR-Co<sub>9</sub>S<sub>8</sub>-I, DR-Co<sub>9</sub>S<sub>8</sub>-II, DR-Co<sub>9</sub>S<sub>8</sub>-III, ST-CoS and ST-CoS<sub>2</sub>.



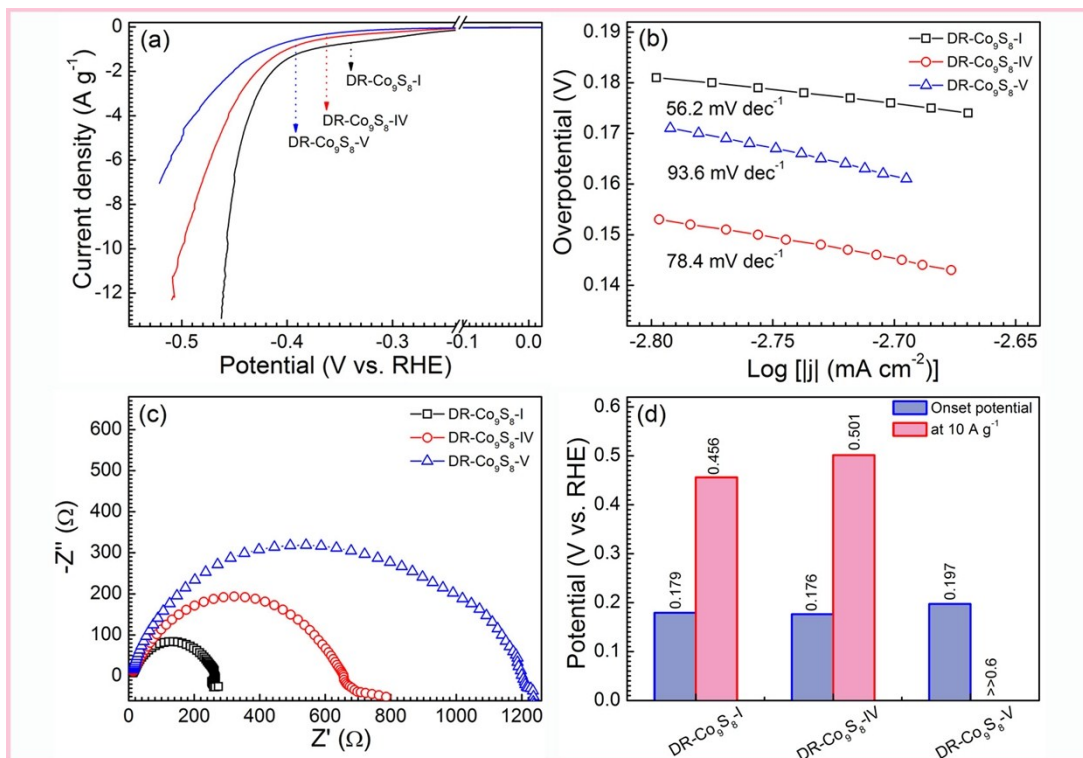


**Figure S6.** (a) Polarization curves, (b) Tafel plots, (c) Nyquist plots, and (d) onset potential of DR-Co<sub>9</sub>S<sub>8</sub>-I, IV, and V.

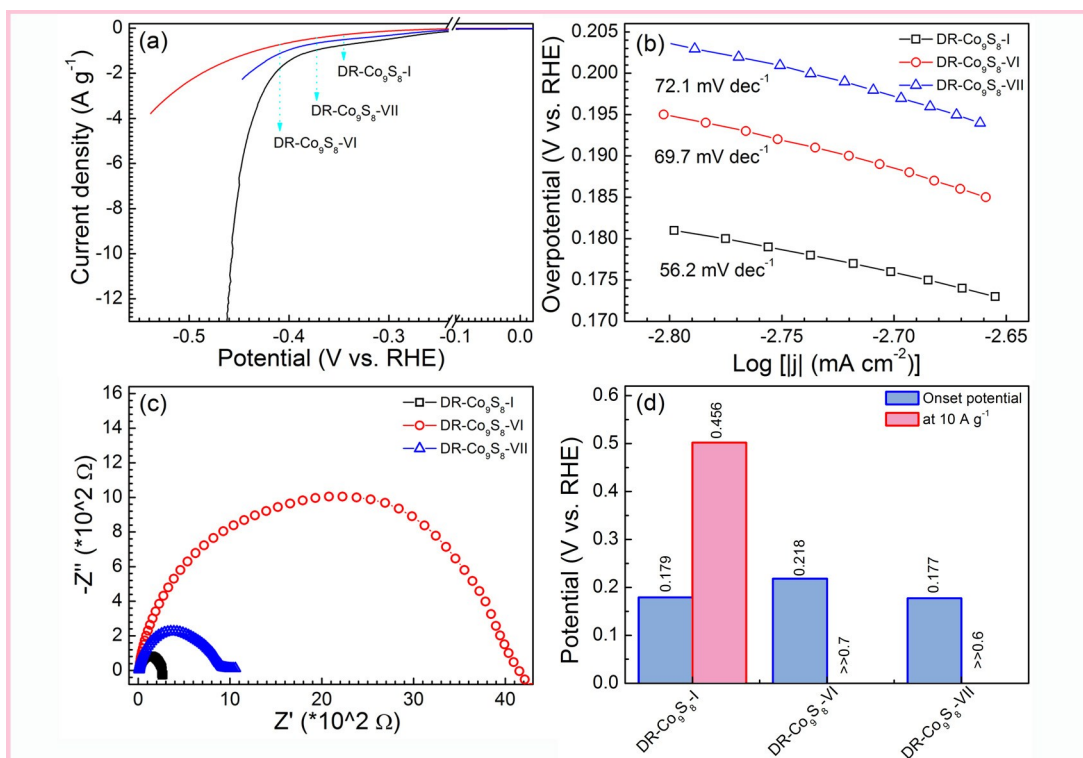


**Figure S7.** (a) Polarization curves, (b) Tafel plots, (c) Nyquist plots, and (d) onset potential of DR-Co<sub>9</sub>S<sub>8</sub>-I, VI, and VII.

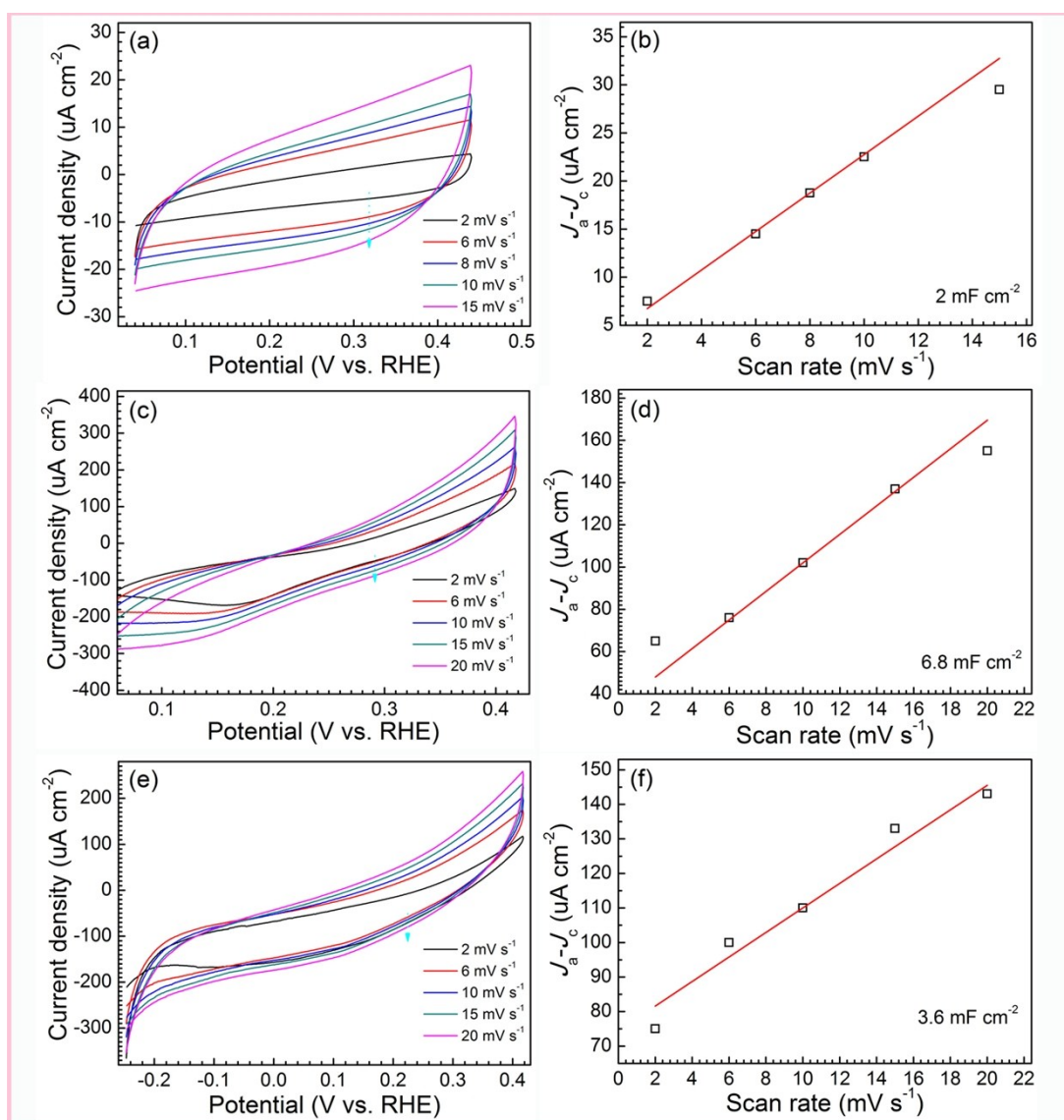


**Figure S8.** (a) Cyclic voltammograms of DR-Co<sub>9</sub>S<sub>8</sub>-II electrode in the approximate region of 0.04-0.44 V vs. RHE at various scan rates, (b) the corresponding linear fitting of the capacitive currents vs. scan rates to estimate the  $C_{dl}$  at -0.22 V vs. RHE, (c) cyclic voltammograms of CoS-ST electrode in the approximate region of -0.26-0.44 V vs. RHE at various scan rates, (d) the corresponding linear fitting of the capacitive currents vs. scan rates to estimate the  $C_{dl}$  at -0.09 V vs. RHE, (e) cyclic voltammograms of CoS<sub>2</sub>-ST electrode in the approximate region of 0.04-0.44 V vs. RHE at various scan rates and (f) the corresponding linear fitting of the capacitive currents vs. scan rates to estimate the  $C_{dl}$  at -0.22 V vs. RHE.



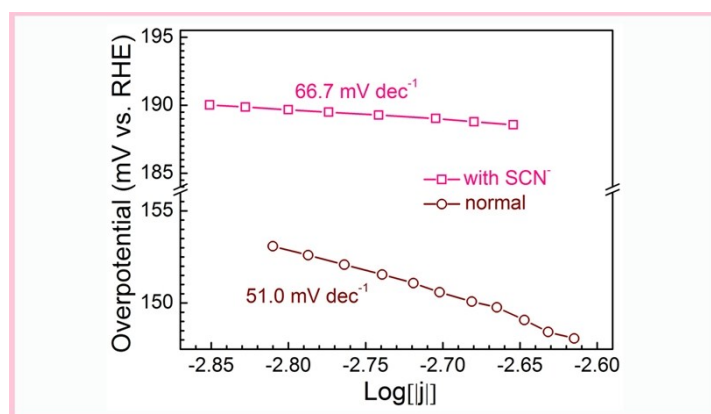


**Figure S9.** The (a) Tafel plots of DR-Co<sub>9</sub>S<sub>8</sub>-II after the addition of SCN<sup>-</sup> ions (10 mM) into 0.5 M H<sub>2</sub>SO<sub>4</sub>.